

Adsorption and dissociation of H₂O on Zr(0001) with density-functional theory studies

Shuang-Xi Wang,^{1,2,3} Ping Zhang,^{3,*} Peng Zhang,⁴ Jian Zhao,⁵ and Shu-Shen Li¹

¹*State Key Laboratory for Superlattices and Microstructures,
Institute of Semiconductors, Chinese Academy of Sciences,
P. O. Box 912, Beijing 100083, People's Republic of China*

²*Department of Physics, Tsinghua University,
Beijing 100084, People's Republic of China*

³*LCP, Institute of Applied Physics and Computational Mathematics,
P.O. Box 8009, Beijing 100088, People's Republic of China*

⁴*Department of Nuclear Science and Technology,
Xi'an Jiaotong University, Xi'an 710049, People's Republic of China*

⁵*State Key Laboratory for Geomechanics and deep underground engineering,
China University of Mining and Technology,
Beijing 100083, People's Republic of China*

Abstract

The adsorption and dissociation of isolated H₂O molecule on Zr(0001) surface are theoretically investigated for the first time by using density-functional theory calculations. Two kinds of adsorption configurations with almost the same adsorption energy are identified as the locally stable states, i.e., the flat and upright configurations respectively. It is shown that the flat adsorption states on the top site are dominated by the $1b_1-d$ band coupling, insensitive to the azimuthal orientation. The diffusion between adjacent top sites reveals that the water molecule is very mobile on the surface. For the upright configuration, we find that besides the contribution of the molecular orbitals $1b_1$ and $3a_1$, the surface→water charge transfer occurring across the Fermi level also plays an important role. The dissociation of H₂O is found to be very facile, especially for the upright configuration, in good accordance with the attainable experimental results. The present results afford to provide a guiding line for deeply understanding the water-induced surface corrosion of zirconium.

PACS numbers: 68.43.Bc, 68.43.Fg, 68.43.Jk, 68.47.De

*Corresponding author; zhang_ping@iapcm.ac.cn

I. INTRODUCTION

The adsorption of water on metal surfaces is of fundamental importance and has gained a lot of interest associated with a variety of phenomena such as heterogeneous catalysis and corrosion of materials [1, 2]. As a result these systems have been intensively investigated by various experimental and theoretical techniques, especially for the transition metal surfaces, such as Cu(100) [3, 4], Fe(100) [5, 6], and Pd(100) [7, 8]. From a practical point of view, it is critical to understand the bonding and orientation characteristics of water molecule on the surfaces. Experimentally, complicated by the facile H₂O cluster formation, it is difficult to discriminate between H₂O monomers and clusters. Thus ambiguities have arisen about the preferred orientation of H₂O molecule on the surfaces.

Theoretically an upright configuration has been proposed for the adsorption of water on metal surfaces [9, 10]. It has been demonstrated that by maximizing the adsorbate-dipole substrate-image-dipole interactions, an upright H₂O favors interaction with the metal surfaces through the molecular orbitals (MOs) of water, mainly $3a_1$ orbital. Nevertheless, in later density-functional theory (DFT) calculations, a flat-lying configuration on the top site of transition metal surfaces has been established by some sophisticated studies [11–13], arguing that the $1b_1$ orbital dominates the water-surface interaction, by coupling with atomic d orbital of the transition metal surfaces. Much desirable it is to handle these conflicting results. To this end, further systematic studies in this area are obviously highly needed for a thorough understanding of the water structures on metal surfaces.

Motivated by this observation, in the present paper we use first-principles calculations to investigate the adsorption properties of H₂O on the Zr(0001) surface. The reason why we choose zirconium as the prototype is that zirconium and its alloys have long been used in nuclear reactors as low neutron adsorption cross-section and excellent corrosion resistance [14]. Water is the main residual gas in the ultrahigh vacuum (UHV) vessels of the nuclear reactors, so it is highly meaningful to study the adsorption of water molecule at zirconium surfaces. The experimental investigations for the adsorption of water on Zr(0001) have been done with various techniques, including low-energy electron diffraction (LEED) [15, 16] and photoemission spectroscopy [17]. Water was found to adsorb on the surface and autocatalytic decomposition took place, as a function of temperature (T) ($170\text{ K} < T < 573\text{ K}$). Despite the experimental results a detailed investigation on the electronic nature of water adsorption and

dissociation on the Zr(0001) surface is indispensable to a complete understanding of water-metal interactions. Moreover, we expect that the present work helps to resolve current existing controversy mentioned above.

Through analysis of the electronic projected density of states (PDOS) and charge density difference, we obtain the adsorption properties of H₂O on the Zr(0001) surface. We find that there exist two kinds of adsorption structures with almost the same adsorption energy as the locally stable states, including flat and upright configurations respectively. It is found that dominated by the $1b_1-d$ band coupling, the flat adsorption states on the top site are insensitive to the azimuthal orientation. The diffusion between adjacent top sites reveals high mobility of the water molecule on Zr(0001). For the upright configuration, we find that besides the hybridization contribution of the molecular orbitals $1b_1$ and $3a_1$, charge transfer between the adsorbate and the substrate near the Fermi energy also plays an important role in electrostatically stabilizing the adsorption structure. Consistent with the attainable experimental measurements, the dissociation of H₂O is found to be very facile, especially for the upright configuration.

The rest of the paper is organized as follows. In Sec. II the computational methods and the supercell models that we use are briefly described. In Sec. III we present and discuss our results for H₂O adsorption on the Zr(0001) surface, followed by diffusion and dissociation properties of the system. Finally, in Sec. IV, we close our paper with a conclusion of our main results.

II. COMPUTATIONAL METHODS

Our calculations are performed within DFT using the Vienna *ab-initio* simulation package (VASP) [18]. The PBE [19] generalized gradient approximation and the projector-augmented wave potential [20] are employed to describe the exchange-correlation energy and the electron-ion interaction, respectively. The cutoff energy for the plane wave expansion is set to 400 eV. The Zr(0001) surface is modeled by a slab composing of five atomic layers and a vacuum region of 20 Å. A 2×2 supercell, in which each monolayer contains four Zr atoms, is adopted in the study of the H₂O adsorption. The water is placed on one side of the slab only and a dipole correction [21] is applied to compensate for the induced dipole moment. During our calculations, the bottom two atomic layers of the Zr substrate

are fixed, and other Zr atoms as well as the H₂O molecule are free to relax until the forces on the ions are less than 0.02 eV/Å. Integration over the Brillouin zone is done using the Monkhorst-Pack scheme [22] with $7 \times 7 \times 1$ grid points. And a Fermi broadening [23] of 0.1 eV is chosen to smear the occupation of the bands around the Fermi level by a finite- T Fermi function and extrapolating to $T = 0$ K.

The calculation of the energy barriers for the water diffusion and dissociation processes is performed using the nudged elastic band (NEB) method [24], which is a method for calculating the minimum energy path between two known minimum energy sites, by introducing a number of “images” along the diffusion path. The energy barrier is determined by relaxing the atomic positions of each image in the direction perpendicular to the path connecting the images, until a force convergence is achieved. In present work, the diffusion path is modeled using seven images, two of which include the minimum energy sites as initial and final positions. As an initial guess, five linearly interpolated, intermediate images between the initial and final configuration are used.

III. RESULTS AND DISCUSSIONS

A. ADSORPTION PROPERTIES

The structural and energetic parameters of the free water molecule are calculated within a box with the same size of the adsorbed systems. The optimized geometry for free H₂O gives a bond length of 0.97 Å and a bond angle of 104.2°, consistent with the experimental values of 0.96 Å and 104.4° [25]. The calculated lattice constant of bulk Zr (a , c) are 3.24 Å and 5.18 Å, respectively, in good agreement with the experimental measurements of 3.233 Å and 5.146 Å [26].

As depicted in Fig. 1(a), we consider four high-symmetry sites on the Zr(0001) surface, respectively the top, bridge (bri), hcp and fcc hollow sites. The O atom of water is initially placed on the precise high-symmetry sites with various orientations of water with respect to the substrate. We find that there exist locally stable adsorption states on the top site of Zr(0001), where the H₂O molecules lie fairly flat on the surface, labeled by employing the notations top- x , $y1$ and $y2$, respectively. Besides, our calculations demonstrate that the upright molecular configuration adsorbed on the bridge site with the O atom lying down is

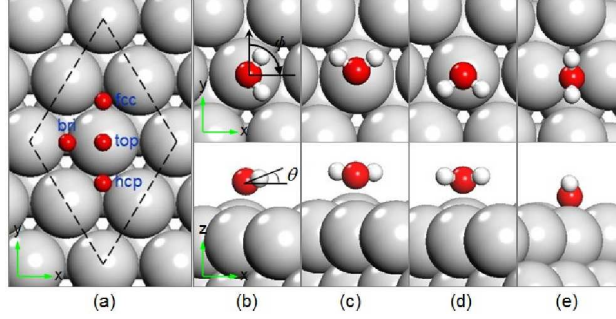


FIG. 1: (Color online) (a) The structure of the $p(2 \times 2)$ surface cell of Zr (0001), and four on-surface adsorption sites, meanwhile the red balls denote the initial positions of O atoms in the adsorption picture. (b)-(e) Top view (upper panels) and side view (lower panels) of the optimized structures of four most stable adsorption states of $\text{H}_2\text{O}/\text{Zr}(0001)$ surface, i.e., top- x , top- $y1$, top- $y2$, and bri- z , respectively. Gray, red and white balls denote Zr, O, and H atoms, respectively.

also a locally state molecular state, labeled by bri- z . The structural and energetic details of the molecular states are illustrated in Figs. 1(b)-(e) and summarized in Table I. In Fig. 1(b) we define two angles ϕ and θ . ϕ represents the azimuthal angle of H_2O with respect to the surface, and θ represents the tilt angle between the H_2O molecular dipole plane and the surface. The adsorption energy of the system is calculated as follows:

$$E_{\text{ad}} = E_{\text{H}_2\text{O}/\text{Zr}(0001)} - E_{\text{H}_2\text{O}} - E_{\text{Zr}(0001)}, \quad (1)$$

where $E_{\text{H}_2\text{O}}$, $E_{\text{Zr}(0001)}$, and $E_{\text{H}_2\text{O}/\text{Zr}(0001)}$ are the total energies of the H_2O molecule, the clean Zr surface, and the adsorption system respectively. According to this definition, a negative value of E_{ad} indicates that the adsorption is exothermic (stable) with respect to a free H_2O molecule and a positive value indicates endothermic (unstable) reaction.

From Table I, we can clearly see that at these stable adsorption sites, the work functions are much smaller than the clean Zr(0001) surface (4.26 eV), implying an observable charge redistribution between the adsorbate water and the surface Zr atoms. Taking the adsorption site top- $y1$ for example, the O-H bond length 0.99 Å is almost identical to 0.97 Å of free H_2O molecule, but the H-O-H bond angle 106.2° is larger than that of free H_2O . The tilt angle is 14.9°, differing a little from that ($\sim 10^\circ$) of other transition metal surfaces mentioned above, where the top site is the most stable state. The adsorption energy -0.616 eV indicates a stronger molecule-surface interaction than on other transition metal surfaces (usually of -0.3

TABLE I: Calculated structural parameters, adsorption energy for a water molecule on Zr(0001) surface. E_a (eV) represents the adsorption energy. Φ (eV) represents the work function. z_O (\AA) represents the vertical height of the O atom from the surface, the height of which is averaged over all atoms on the surface. d_{O-H} (\AA) represents the bond length between the O and H atoms. θ ($^\circ$) represents the tilt angle between the H_2O molecular dipole plane and the surface. $\alpha_{\text{H-O-H}}$ ($^\circ$) represents the H-O-H bond angle.

Site	E_a	Φ	z_O	d_{O-H}	θ	$\alpha_{\text{H-O-H}}$
top- x	-0.611	3.35	2.35	0.99	16.8	105.9
top- $y1$	-0.616	3.38	2.35	0.99	14.9	106.2
top- $y2$	-0.609	3.35	2.34	0.99	15.9	106.1
bri- z	-0.610	2.94	1.88	0.99	90.0	110.6

eV). For the adsorption site bri- z , a lower work function 2.94 eV and a larger H-O-H bond angle 110.6° are identified, suggesting more prominent charge redistribution and molecular distortion compared to the top-site adsorption. It is clear that the bri- z adsorption almost has the same adsorption energy as the top-site adsorption. This is quite different from previous DFT calculations on other transition metal surfaces that predicted the flat-lying top-site adsorption to be the most stable configuration. Interestingly, for a H_2O molecule to reach the adsorption state, there does not exist any energy barrier, which means that H_2O can be adsorbed on the Zr(0001) surface spontaneously.

As presented in Table I, the energetic differences among these three adsorption states on top site are very tiny. For further illustration, we investigate the azimuthal orientation of the adsorbed H_2O , which is shown in Fig. 2. It can be seen that the adsorption site top- $y1$ is slightly more stable. Nevertheless, it is noted that the variation of the adsorption energy for different azimuthal orientations are determined to be less than 0.01 eV. We will see below that this is much smaller than the energy barrier of the lateral diffusion, implying that the azimuthal rotation is essentially unhindered and may occur at very low temperature.

In order to further understand the precise nature of the chemisorbed molecular state, the electronic PDOS of the H_2O molecule and the topmost Zr layer are calculated. As typical examples, here we plot in Fig. 3 the PDOS for the stable adsorption configurations of top- $y1$

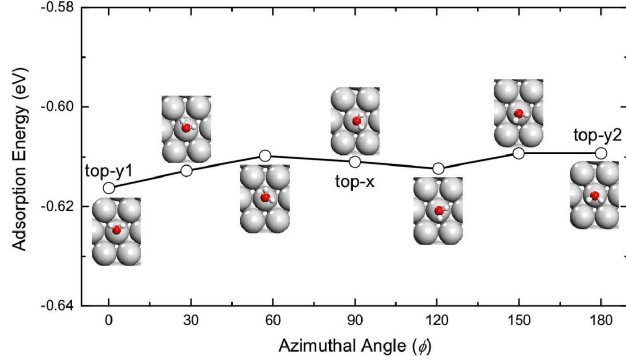


FIG. 2: (Color online) Calculated adsorption energy of H_2O as a function of the azimuthal angle at the top site. The insets show the structures adopted in the calculations.

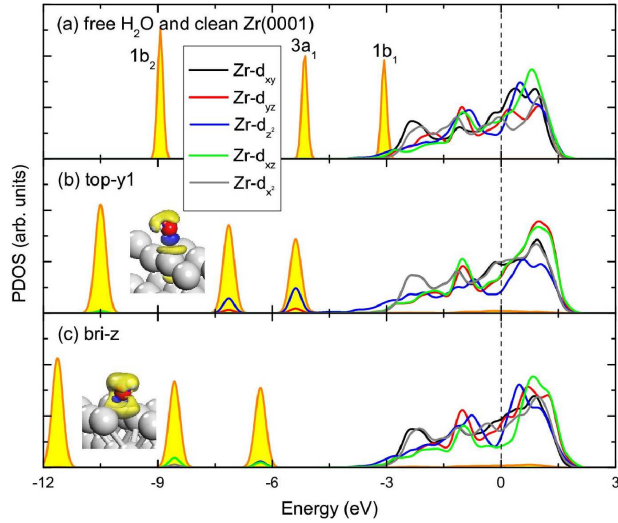


FIG. 3: (Color online) The PDOS of the H_2O molecule and the top-layer Zr atom bonded to H_2O for (a) free H_2O and the clean $\text{Zr}(0001)$ surface, (b) top- $y1$ adsorption site and (c) bri- z adsorption site. The insets in (b) and (c) show the 3D electron density difference, with the isosurface value set at $\pm 0.015 e/\text{\AA}^3$. The area filled with yellow color represents molecular orbital of H_2O . The Fermi level is set to zero.

and bri- z . For comparison, the PDOS of the free H_2O molecule and clean $\text{Zr}(0001)$ surface are also shown in Fig. 3(a). The three-dimensional (3D) electron density difference $\Delta\rho(\mathbf{r})$, which is obtained by subtracting the electron densities of noninteracting component systems, $\rho^{\text{Be}(0001)}(\mathbf{r}) + \rho^{\text{H}_2\text{O}}(\mathbf{r})$, from the density $\rho(\mathbf{r})$ of the $\text{H}_2\text{O}/\text{Zr}(0001)$ surface, while retaining the atomic positions of the component systems at the same location as in $\text{H}_2\text{O}/\text{Zr}(0001)$,

is also shown in the insets of Fig. 3. Positive (blue) $\Delta\rho(\mathbf{r})$ indicates accumulation of electron density upon binding, while a negative (yellow) one corresponds to electron density depletion. MOs $2a_1$ and $1b_2$ of water (not shown here) are far below the Fermi level and thus remain intact in water-metal interaction. Here we consider only three MOs $1b_2$, $3a_1$, and $1b_1$.

In the case of adsorption on the top- $y1$ site, as illustrated in Fig. 3(b), these three MOs are rigidly shifted downward by 1.57, 2.02 and 2.33 eV, respectively. This is essentially caused by the different electronegativities of Zr and water molecule, which induces charge redistribution and thus build a global electrostatic attraction between the water and substrate. In addition to this rigid energy shift, it is also noticeable that due to the molecule-metal orbital hybridization, the MOs of adsorbed water are broadened apparently for $1b_1$ and $3a_1$, which are known to have an oxygen lone-pair character perpendicular to the molecular plane, and a mixture of partial lone-pair character parallel to the molecular plane and partial O-H bonding character, respectively [1, 6]. Remarkably, the water adsorption introduces new peaks for both d_{z^2} and d_{yz} states of the surface Zr atom, aligning in energy with $1b_1$ and $3a_1$. Especially for $1b_1$, more electronic states of the Zr atom, mostly d_{z^2} appear nearby, indicating that the adsorbed $1b_1$ MO may act as an electron donor state. This is quite in accordance with the general picture that the water-surface interaction is dominated by the $1b_1$ - d band coupling. It is obvious that this kind of coupling cannot be effected essentially by the azimuthal rotation of the water, hence the adsorption of H_2O on the top site is insensitive to the azimuthal orientation. The features of the orbital hybridization are further substantiated by the 3D electron density difference plotted in the inset of Fig. 3(b), from which we can see that there exists a large charge accumulation between the adsorbate and substrate.

For upright adsorption site bri-z [Fig. 3(c)], it is known that $3a_1$ plays an additional key role in the upright adsorption structure of water monomer [11]. Here obviously, the orbital $3a_1$ undergoes a noticeable broadening as well as $1b_1$. We notice that instead of d_{yz} , it is the state d_{xz} of the Zr atom, together with d_{z^2} , that overlaps with the orbital $1b_1$ of water. And new peaks for d_{xz} and d_{x^2} emerge aligning in energy with the orbital $3a_1$. This observable overlapping can also be seen from the 3D electron density difference plotted in the inset of Fig. 3(c), from which we find a large charge accumulation between the O atom and two adjacent top-layer Zr atoms. Moreover, it is noteworthy that a discernible occupied domain

of states of the adsorbed water emerges near the Fermi level, suggesting more prominent charge transfer between adsorbate and substrate than the top-site adsorption. We find that the emerged occupied state aligns with the lowest unoccupied MO, which coincides with the so-called Blyholder model [27], where an electron donation from the adsorbate highest occupied MO to substrate states and a back-donation from such states to the lowest unoccupied MO of the adsorbate build up the chemisorption bond. With a distortion of the adsorbed water, the MOs are shifted down by 2.70, 3.43 and 3.25 eV for $1b_2$, $3a_1$ and $1b_1$, respectively, which are more pronounced compared with those on top- $y1$, especially for the orbital $3a_1$, hence more unoccupied MOs are drawn below the Fermi level. Therefore, although observable is the overlapping, charge transfer is more prominent for the bri- z adsorption, leading to a considerable stable electrostatic bonding between water and the surface.

B. DIFFUSION OF H₂O MOLECULE

Given a H₂O molecule at a stable adsorption site, it is interesting to see how it diffuses on the substrate. Here, therefore, we calculate the diffusion paths and energetic barriers of water on Zr(0001) surface between neighboring adsorption sites along the top- x , top- $y1$ and top- $y2$ channels respectively, which are schematically shown in the insets of Fig. 4. Each lateral diffusion path adopted here connects two minimum energy states on the top sites, through the bridge site as a transition state. The adsorption energies as a function of the lateral displacement of O atom are shown in Fig. 4.

For the channel top- $y1$, the transition state with the energy maximum located on the bridge site, which is not a stable adsorption site. It is found that the water molecule moves towards the adjacent top- $y1$ site straightforwardly, with slight wiggling along the diffusion path. Moreover, the diffusion energy barrier 0.315 eV along this path is much lower than the adsorption energy on top- $y1$ site, implying that the water molecule has a high mobility on the Zr(0001) surface. This is the same trend that is found for the channel top- $y2$, with a lower barrier 0.280 eV.

In the case of channel top- x , the lower diffusion barrier 0.061 eV indicates a higher mobility than that along those fore-mentioned two channels. Furthermore, there exists a local energy minimum along this diffusion path. Investigation in more detail in this particular

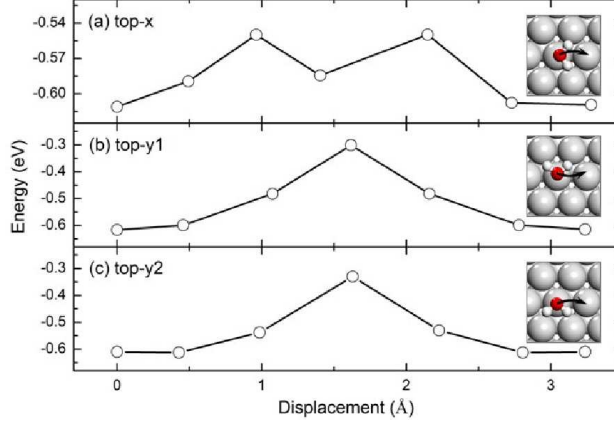


FIG. 4: (Color online) Diffusion of H_2O on the top site of $\text{Zr}(0001)$ surface as a function of the lateral displacement of O atom from its original site top- x (upper panel), top- $y1$ (middle panel), and top- $y2$ (lower panel), respectively.

case reveals that this energy minimum coincides with the stable bridge adsorption site bri- z , which means that the water molecule may rotate during the diffusion. We find that as the water molecule migrates towards the adjacent top site, it rotates around the O atom and overcomes an energy barrier, till the tilt angle reaches as high as 71° , where the molecule moves to the bridge site as a transition state. Then the water molecule rotates reversely, overcoming another barrier and arriving at the adjacent top- x site. This energy minimum state located on the bridge site may also give a reason why this channel possesses the lowest diffusion barrier.

The energy barriers of these lateral diffusion channels are larger than that of the azimuthal rotations mentioned above, whereas by assuming the attempt frequency 10^{13} of the adsorbate, the energy barriers of these three diffusion channels top- x , top- $y1$ and top- $y2$ correspond to temperature of about 24, 122, and 109 K, respectively, suggesting that the diffusion can occur under room temperature on the $\text{H}_2\text{O}/\text{Zr}(0001)$ surface, especially for the channel top- x . These results provide evidence that the water molecules are very mobile on $\text{Zr}(0001)$, even at very low temperature [28].

C. DISSOCIATION OF H₂O MOLECULE

Finally let us discuss the possibility of dissociation of H₂O molecule into H and OH species on the Zr(0001) surface. In order to investigate the water dissociation process, we begin with the adsorption properties of the dissociated H and OH species. The structural and energetic details of these species are summarized in Table II. For the H species, the hcp site is the most stable with an adsorption energy of -3.298 eV, and the fcc site is slightly less stable with an adsorption energy of -3.240 eV. Next, for the OH species, the most stable site is found to be fcc with an adsorption energy of -5.627 eV, and the hcp site is less stable by 0.086 eV than the fcc site. The O-H bond length (0.98 Å) with O atom end-on orientation is less than that (1.00 Å) of the free OH molecule.

TABLE II: Calculated structural parameters, adsorption energy for water dissociation products on Zr(0001) surface. E_a (eV) represents the adsorption energy. z (Å) represents the vertical height of the H atom (for H species) or O atom (for OH species) from the surface.

Species	Site	E_a	z	$d_{\text{O-H}}$
H	hcp/fcc	-3.298/-3.240	1.13/1.09	
OH	fcc/hcp	-5.627/-5.541	1.32/1.33	0.98/0.98

TABLE III: Calculated structural parameters, adsorption energy for the final H+OH configurations and the dissociation barriers of water molecule on Zr(0001) surface. E_d (eV) represents the dissociation barrier. Site_H and Site_OH represent the positions of H and OH species in the dissociative configuration, respectively.

Path	E_a	E_d	Φ	Site_H	Site_OH	z_H	z_O	$d_{\text{O-H}}$
top- x	-8.288	0.106	3.16	fcc	hcp	1.07	1.34	0.97
top- $y1$	-8.288	0.261	3.16	fcc	hcp	1.07	1.34	0.97
top- $y2$	-8.462	0.371	3.18	hcp	fcc	1.09	1.38	0.97
bri- z	-8.288	0.093	3.16	fcc	hcp	1.07	1.34	0.97

We examine four probable dissociation paths of H₂O molecule on the Zr(0001) surface.

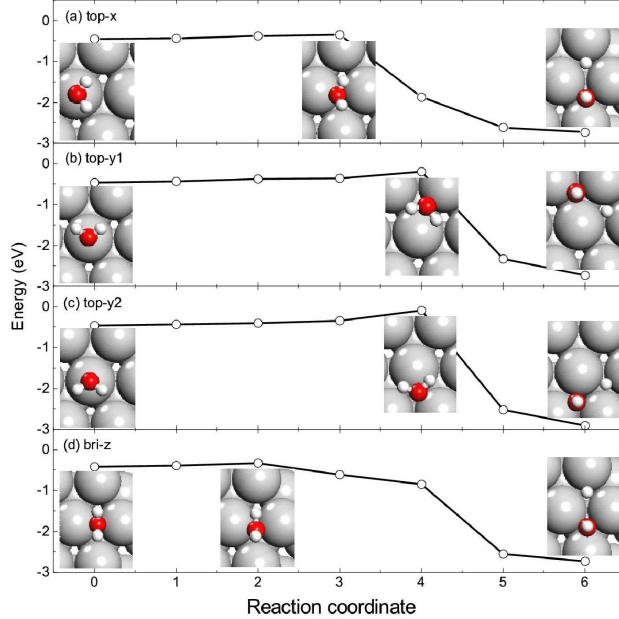


FIG. 5: (Color online) Four water dissociation paths considered in this study, corresponding to the four most stable adsorption states represented in Fig. 1. The inset pictures show the structures of $\text{H}_2\text{O}/\text{Zr}(0001)$ surface corresponding to the adsorption, transition and dissociation states, respectively.

The initial states as the precursors for dissociation are four stable molecular adsorption states discussed above. For the final states, based on the results of the adsorption of H and OH, we consider several possible combinations of the adsorption sites for H and OH species. It is found that for the H+OH configuration, the H and OH species occupy two neighboring hollow sites (fcc and hcp) respectively connected via a bridge site, which is the most stable. Table III shows the structural and energetic details of the final H+OH configurations. We can see from the low adsorption energies and work functions that these two species strongly bond to the surface, with OH oriented almost perpendicular to the surface. The O–H bond length 0.97 \AA differs only slightly from that of the adsorbed H_2O molecule.

Figure 5 shows the energy profiles for these dissociation paths. The activation energies for the dissociation of the water molecules are 0.093, 0.106, 0.261 and 0.371 eV along the paths bri-z, top-x, top-y1 and top-y2, respectively (see Table III). We find that the paths top-x and bri-z have noticeably low dissociation barriers, small enough to facilitate the dissociations of the adsorbed water molecules. While for the paths top-y1 and top-y2, the energy barriers are

higher than that of the forenamed two paths. The reason why such differences exist about the energy barriers will be clear when we go deep into the dissociation process. For the path bri- z , it can be seen (from the inset pictures of Fig. 5) that the water molecule starts to dissociate almost *in situ*, hence the energy barrier is low. In the case of path top- x , the water molecule first migrates to the adjacent bridge site, meanwhile the molecule rotates around the O atom for a larger tilt angle (which it can do with little energy loss), then following the dissociation process just as in the path bri- z . On the other hand, for the dissociation paths top- $y1$ and top- $y2$, before reaching the transition states, the water molecules have to rotate more complexly, then enter the dissociation process with the H and OH species moving to their final positions. By assuming the attempt frequency 10^{13} of the adsorbate, the energy barriers of these four dissociation paths correspond to temperature of about 36, 41, 101 and 144 K, respectively, suggesting that the dissociation can occur under room temperature on the H₂O/Zr(0001) surface, especially for the path bri- z . This is in good accordance with the experimental observations that water can spontaneously dissociate on the Zr(0001) surface [16, 17], but different from the dissociation of water on other transition metal surfaces such as Fe(100) [6], Rh(111) and Ni(111) [29], which need to overcome much higher barriers.

IV. CONCLUSIONS

In conclusion, we have systematically studied the adsorption and dissociation behaviors of H₂O on the Zr(0001) surface by using first-principles DFT method. Two kinds of adsorption structures with almost the same adsorption energy were identified as the locally stable states, i.e., the flat and upright configurations respectively. It has been shown that the flat adsorption states on the top site are dominated by the interaction between the water MO $1b_1$ and the metal d band, insensitive to the azimuthal orientation. The diffusion of water across the surface reveals that the adsorbed water is very mobile on the surface. For the upright configuration, we have found that the hybridization between the d band of the Zr(0001) surface and MOs $1b_1$ and $3a_1$ of the water, as well as the charge transfer between the adsorbate and the substrate, contribute to the adsorption system. Consistent with previous experimental results, the dissociation of H₂O has been found to be very facile, especially for the upright configuration. We expect that the present results are greatly helpful for the

practical usage of zirconium in nuclear reactors.

- [1] P. A. Thiel and T. E. Madey, *Surf. Sci. Rep.* **7**, 211 (1987).
- [2] M. A. Henderson, *Surf. Sci. Rep.* **46**, 1 (2002).
- [3] R. Brosseau, M. R. Brustein, and T. H. Ellis, *Surf. Sci.* **294**, 143 (1993).
- [4] S. Wang, Y. Cao, and P. A. Rikvold, *Phys. Rev. B* **70**, 205410 (2004).
- [5] W.-H. Hung, J. Schwartz, and S. L. Bernasek, *Surf. Sci.* **248**, 332 (1991).
- [6] S. C. Jung and M. H. Kang, *Phys. Rev. B* **81**, 115460 (2010).
- [7] K. G. Lloyd, B. A. Banse, and J. C. Hemminger, *Phys. Rev. B* **33**, R2858 (1986).
- [8] J. Li, S. Zhu, Y. Li, and F. Wang, *Phys. Rev. B* **76**, 235433 (2007).
- [9] S. Seong and A. B. Anderson, *J. Phys. Chem.* **100**, 11744 (1996).
- [10] K. Morgenstern and K. H. Rieder, *J. Chem. Phys.* **116**, 5746 (2002).
- [11] A. Michaelides, V. A. Ranea, P. L. de Andres, and D. A. King, *Phys. Rev. Lett.* **90**, 216102 (2003).
- [12] S. Meng, E. G. Wang, and S. Gao, *Phys. Rev. B* **69**, 195404 (2004).
- [13] J. Carrasco, A. Michaelides, and M. Scheffler, *J. Chem. Phys.* **130**, 184707 (2009).
- [14] N. Stojilovic, E. T. Bender, R. D. Ramsier, *Progress in Surface Science* **78**, 101 (2005).
- [15] B. Li, K. Griffiths, C.-S. Zhang, and P.R. Norton, *Surf. Sci.* **370**, 97 (1997).
- [16] B. Li, K. Griffiths, C.-S. Zhang, and P.R. Norton, *Surf. Sci.* **384**, 70 (1997).
- [17] V. Dudr, F. S. utara, T. Skála, M. Vondráček, N. Tsud, V. Matolín, K.C. Prince, and V. Cháb, *Surf. Sci.* **600**, 3581 (2006).
- [18] G. Kresse and J. Furthmuller, *Phys. Rev. B* **54**, 11169 (1996).
- [19] J. P. Perdew, K. Burke, and M. Ernzerhof, *Phys. Rev. Lett.* **77**, 3865 (1996).
- [20] G. Kresse and D. Joubert, *Phys. Rev. B* **59**, 1758 (1999).
- [21] L. Bengtsson, *Phys. Rev. B* **59**, 12301 (1999).
- [22] H. J. Monkhorst and J. D. Pack, *Phys. Rev. B* **13**, 5188 (1976).
- [23] M. Weinert and J.W. Davenport, *Phys. Rev. B* **45**, 13709 (1992).
- [24] H. Jónsson, G. Mills, and K. W. Jacobsen, in *Classical and Quantum Dynamics in Condensed Phase Simulations*, edited by B. J. Berne et al. (World Scientific, Singapore, 1998).
- [25] D. Eisenberg and W. Kauzmann, *The Structure and Properties of Water* (Oxford University

Press, New York, 1969).

- [26] Y. S. Zhao, J. Z. Zhang, C. Pantea, J. Qian, L. L. Daemen, P. A. Rigg, R. S. Hixson, G. T. Gray III, Y. P. Yang, L. P. Wang, and T. Y. Uchida, *Phys. Rev. B* **71**, 184119 (2005).
- [27] G. Blyholder, *J. Phys. Chem.* **68**, 2772 (1964).
- [28] T. Mitsui, M.K. Rose, E. Fomin, D.F. Ogletree, and M. Salmeron, *Science* **297**, 1850 (2002).
- [29] M. Pozzo, G. Carlini, R. Rosei, and D. Alfè, *J. Chem. Phys.* **126**, 164706 (2007).